Space Weather effects observed on the ground
– geomagnetic effects –

J. Watermann
Danish Meteorological Institute, Copenhagen, Denmark

my thanks to

Ground-based systems affected by space weather

(physics oriented categories)

- long-distance communication cables
- gas and oil pipelines
- electric power supply grids

sensitive to the time derivative $\partial B/\partial t$

- magnetic anomaly surveys (e.g., aeromagnetic surveys)
- directional well drilling

affected by the amplitude δB

Ground-based systems affected by space weather

(technical and economical categories)

- gas and oil pipelines *(long-term or cumulative effects)*
- electric power supply grids (*single-event upsets*)

may suffer equipment damage under adverse conditions

- long-distance communication cables
- magnetic anomaly surveys (e.g., aeromagnetic surveys)
- directional drilling operations

no direct damage but operation possibly impeded

First physics category

equipment sensitive to the time derivative $\partial B/\partial t$

- long-distance communication cables
- gas and oil pipelines
- electric power supply grids

problems can arise from geomagnetically induced currents

Medford et al., Geomagnetic induction on a transatlantic communications cable, Nature 290, 392, 1981

Medford et al., Transatlantic earth potential variations during the March 1989 magnetic storms, Geophys. Res. Lett., 16(10), 1145, 1989

Lanzerotti et al., Response of large-scale geoelectric fields to identified interplanetary disturbances and the equatorial ring current, Adv. Space Res., 26(1), 21, 2000

Lanzerotti, Space weather effects on communications, Space Storms and Space Weather Hazards, NATO Science Series II-38, Kluwer, 313, 2001 *(ranges from telegraph to satellite communication)*

Campbell, Observation of electric currents in the Alaska oil pipeline resulting from auroral electrojet current sources, Geophys. J. R. astr. Soc., 61, 437, 1980

Campbell, An interpretation of induced electric currents in long pipelines caused by natural geomagnetic sources of the upper atmosphere, Surveys in Geophysics, 8, 239, 1986

Boteler, Geomagnetic effects on the pipe-to-soil potentials of a continental pipeline, Adv. Space Res., 26(1), 15, 2000

Pulkkinen et al., Recordings and occurence of geomagnetically induced currents in the Finnish natural gas pipeline network, J. App. Geo., 48, 219, 2001

Viljanen & Pirjola, Geomagnetically induced currents in the Finnish high voltage power system, Surveys in Geophysics, 15, 383, 1994

Boteler et al., The effects of geomagnetic disturbances on electrical systems at the Earth's surface, Adv. Space Res., 22(1), 17, 1998 *(includes appendix with list of historic GIC events)*

Pirjola et al., Prediction of geomagnetically induced currents in power transmission systems, Adv. Space Res., 26(1), 5, 2000

Kappenman, An introduction to power grid impacts and vulnerabilties from space weather, Space Storms and Space Weather Hazards, NATO Science Series II-38, Kluwer, 335, 2001

Kappenman, Space weather and the vulnerability of electric power grids, Effects of Space Weather on Technology Infrastructure, NATO Science Series, II-176, Kluwer, 257, 2004

Béland & Small, Space weather effects on power transmission systems: the cases of Hydro-Québec and Transpower New Zealand Ltd, Effects of Space Weather on Technology Infrastructure, NATO Science Series, II-176, Kluwer, 287, 2004

Boteler, Geomagnetic hazards to conducting networks, Natural Hazards 28, Kluwer, 537, 2003

Geomagnetic induction:

basic physical principles

$$\nabla \times E = -\frac{\partial B}{\partial t} \qquad \nabla \times B = \mu_0 \left(j + \frac{\partial D}{\partial t} \right)$$

$$\nabla \cdot D = \rho \qquad \nabla \cdot B = 0$$

$$j = \sigma E$$

$\mu = \mu_0$ $\sigma \equiv$ uniform and finite $\rho \cong 0$

restricted to ULF & ELF band

$\Downarrow$

diffusion equation

$$\nabla^2 E = \mu_0 \sigma \frac{\partial E}{\partial t} \qquad \nabla^2 B = \mu_0 \sigma \frac{\partial B}{\partial t}$$

assume harmonic plane wave source field

$$E_x^2 = \frac{\omega}{\mu_0 \sigma} B_y^2 \qquad j_x^2 = \frac{\sigma \omega}{\mu_0} B_y^2$$

amplitude reduced to 1/e at depth

$$d = \sqrt{\frac{2}{\mu_0 \sigma \omega}}$$

Long-distance communication cables,
specifically transoceanic cables

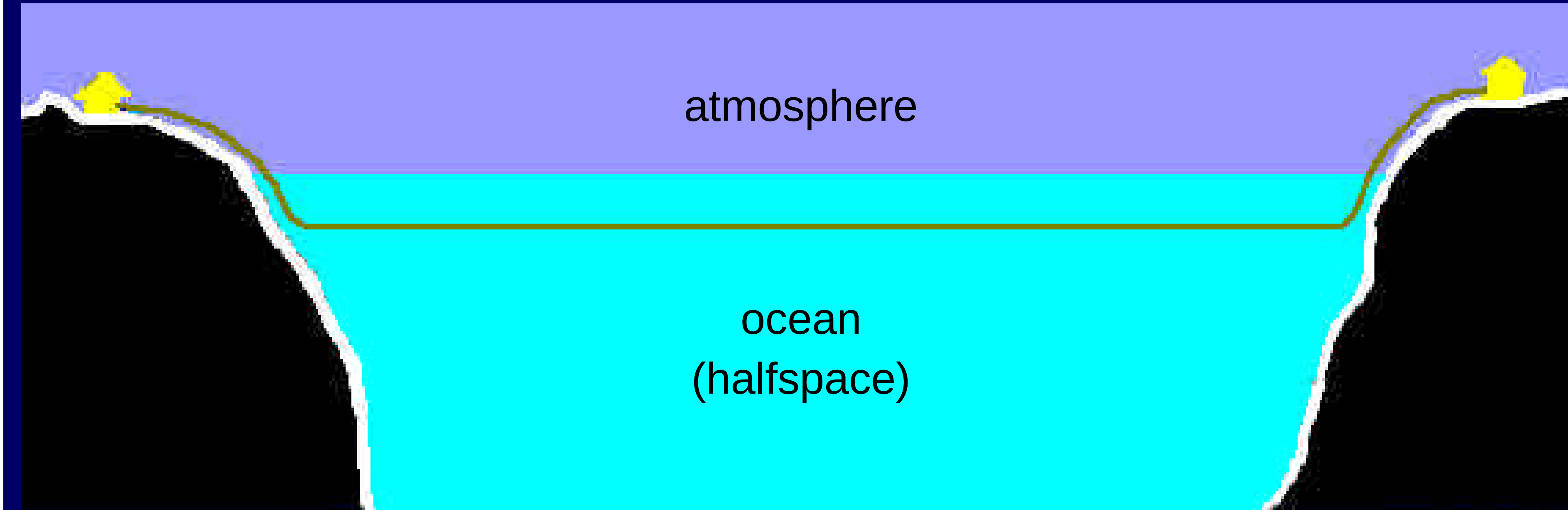

unrealistic situation

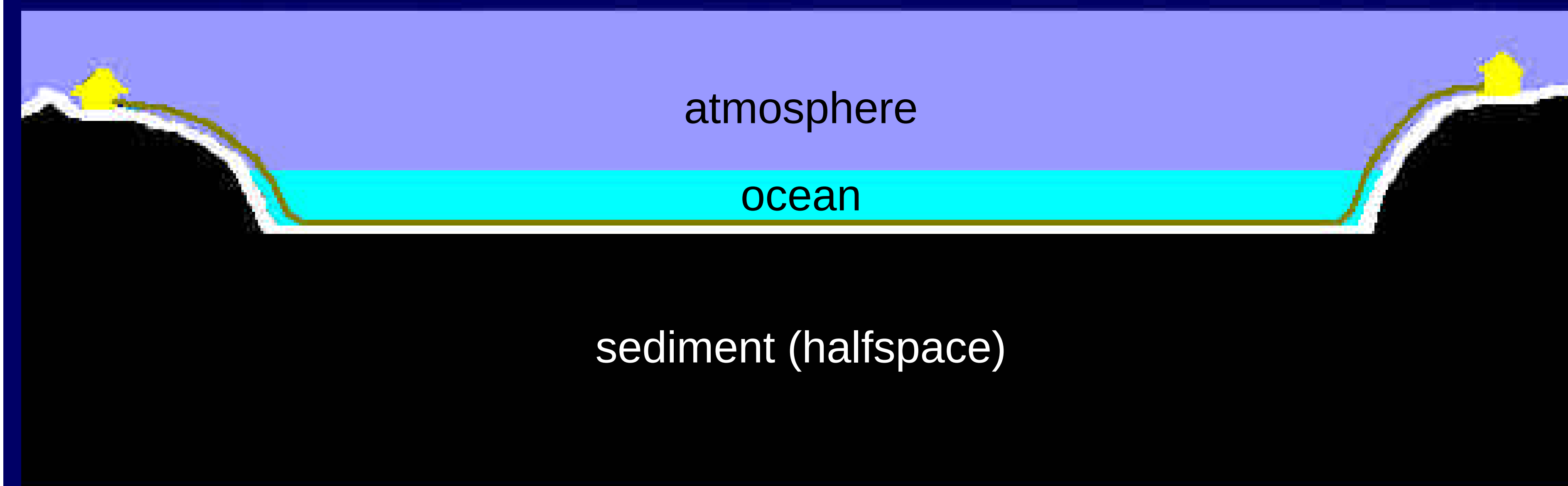

more (but not entirely) realistic situation

Magnetic field amplitude: sea bottom *vs.* sea surface

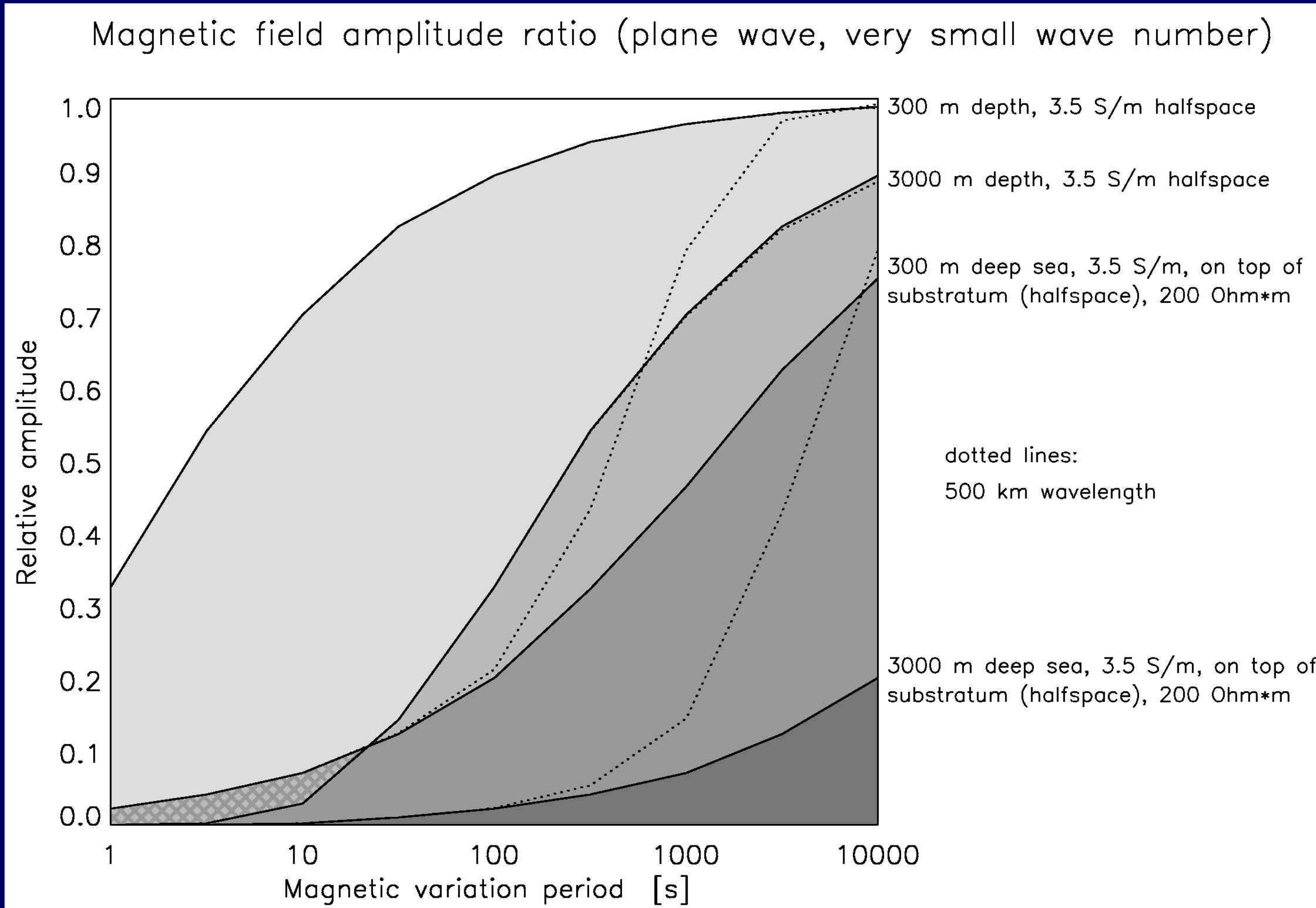

computed after Schmucker, Anomalies of geomagnetic variations in the Southwestern United States, Bull. Scripps Inst. Oceanogr. 13, 1970

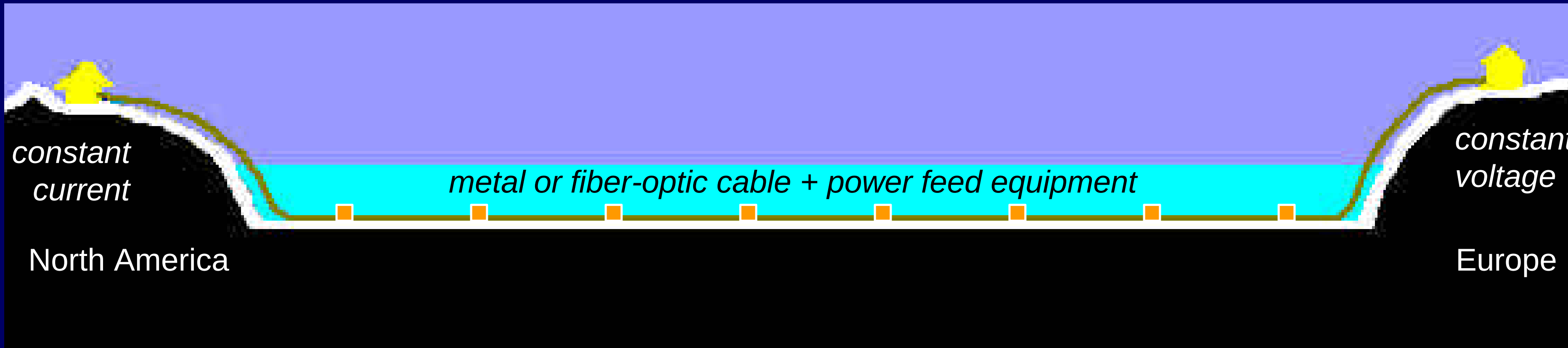

TransAtlantic Telecommunications (TAT) cables

	event	voltage excursion
TAT-6 (*electric*)	Sq	~5 V
TAT-7 (*electric*)	10/19/84	~30 V
TAT-7	04/21/85	~60 V
TAT-8 (*optic* + *PFE*)	ssc 03/13/89	~75 V
TAT-8	03/13/89, 1110 UT	~300 V
TAT-8	03/13/89, 2145 UT	~450 V
TAT-8	03/14/89, 0130 UT	~700 V

table after Medford et al., GRL 16, 1989

Gas and oil pipelines

Pipeline problem: corrosion through induction

must be kept away from steel pipe

$$H_2O \Rightarrow H^+ + OH^-$$

$$Fe^{++} + 2\,(OH)^- \Rightarrow Fe(OH)^2$$

$$Fe^{+++} + 3\,(OH)^- \Rightarrow Fe(OH)^3$$

Rust is formed if the cathodic potential exceeds the safety limit of about 850–1150 mV (negative pipe potential with respect to surrounding soil). Pipelines bends are particularly vulnerable.

However, the problem exists only if

(1) the (normally insulating) pipe coating is damaged, and

(2) the chemical reaction lasts long enough or is frequently repeated

Large area electric power supply nets

best known

"Hydro-Québec blackout"

1989-03-13, 07:45 UT

lasted 9 hours in some parts

affected eastern Canada and northeastern USA

---

more recent and less known outside Europe

"Malmö blackout"

2003-10-30, 20:07 UT

lasted 20-50 min

affected various parts of southern Sweden

Magnetospheric background

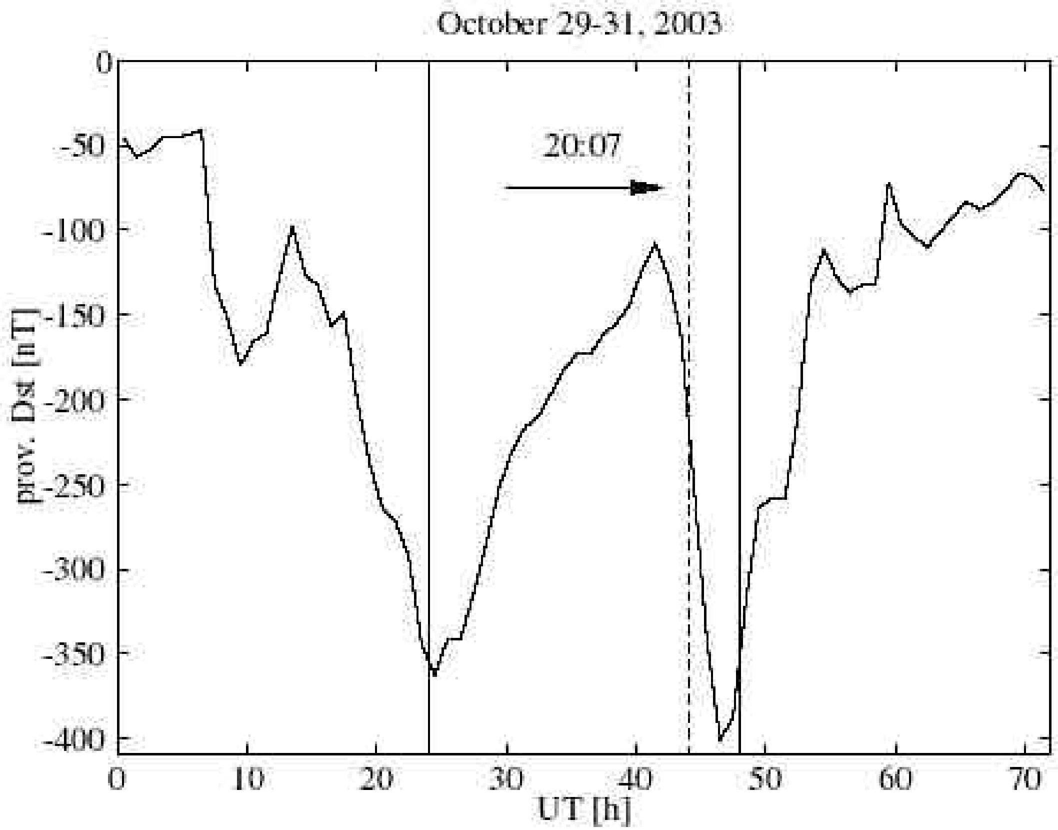

Figure 4: Provisional D_{st} on October 29-31, 2003. The blackout occurred during the increasing phase of the storm.

figure from Viljanen et al., ICS-7,2004

plane wave induced electric field assuming a 100 Ω·m halfspace

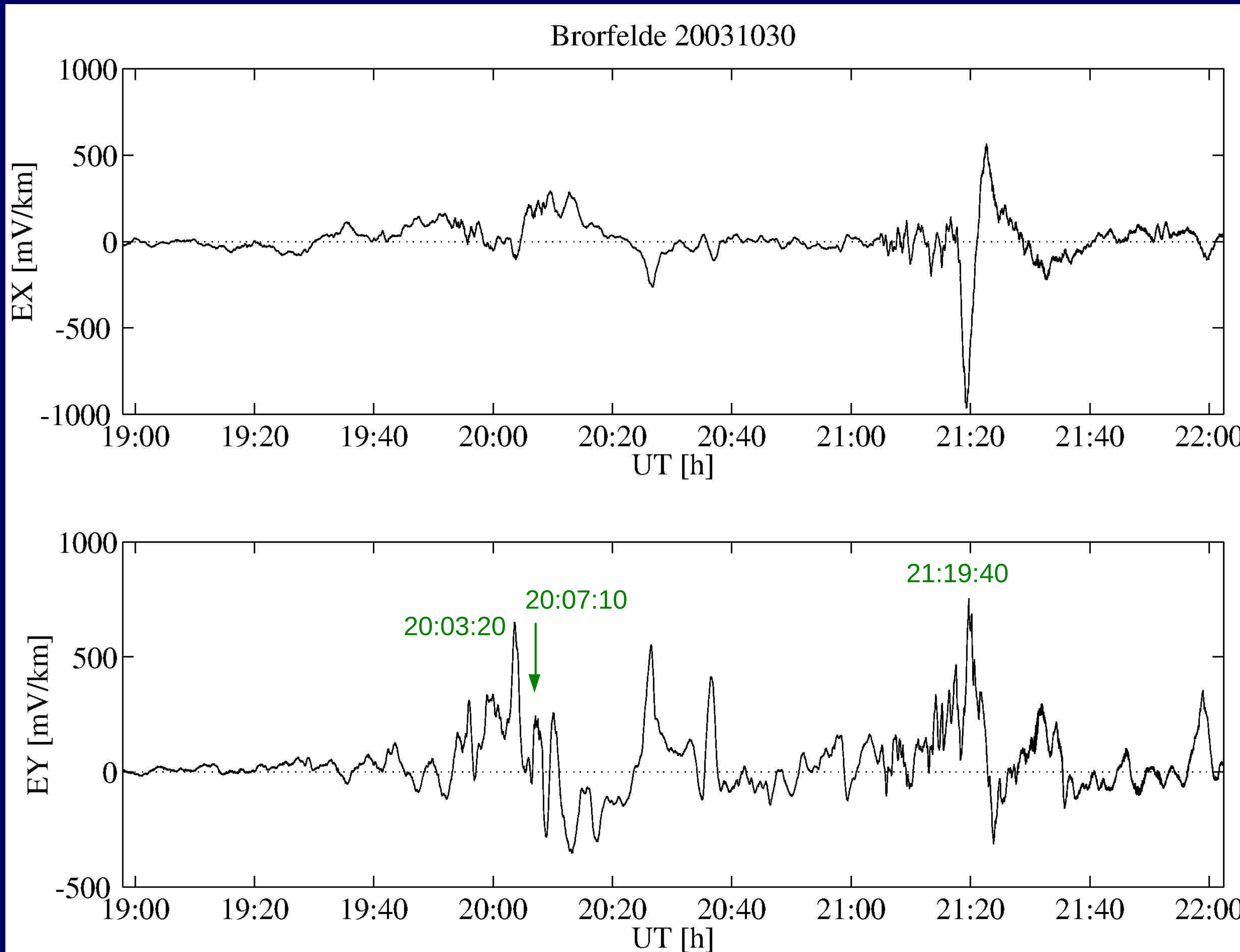

figure compiled by A.Viljanen, 2004

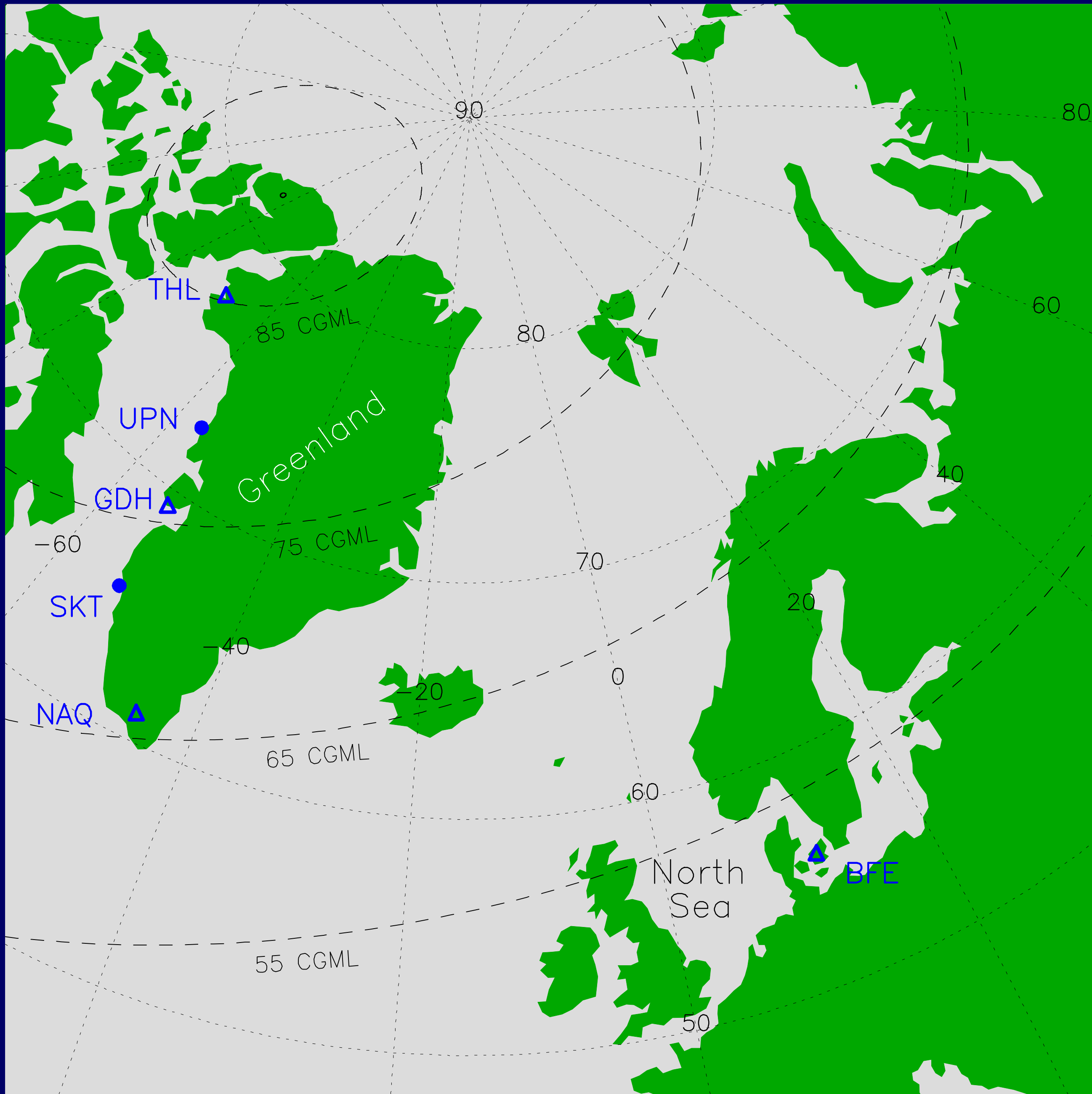

Geomagnetic observatories and selected variometer stations operated by DMI

Brorfelde:

MLT @ UT + 1.7 hrs

Greenland west coast:

MLT @ UT – 2.4 hrs

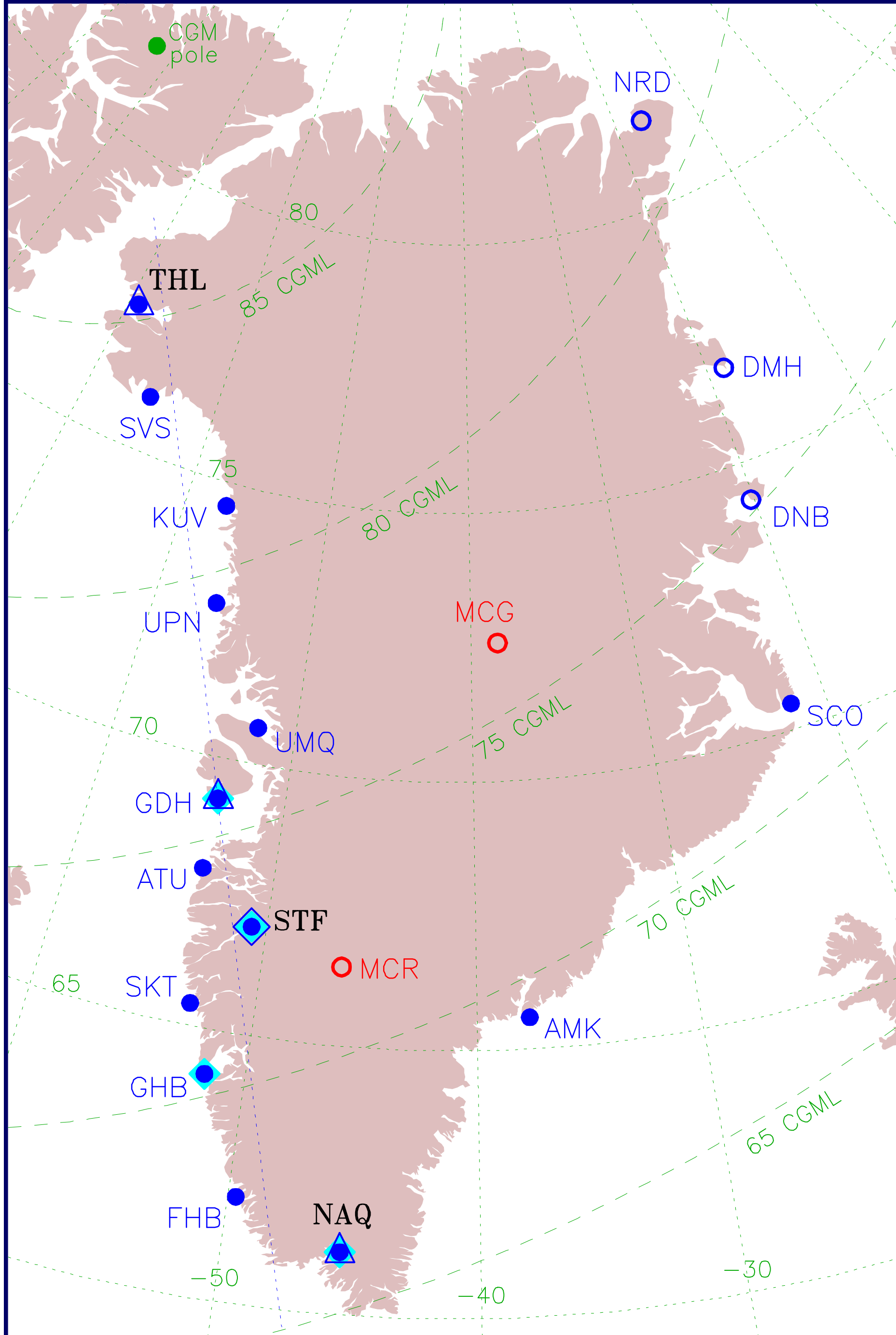

Greenland Magnetometry

Dotted grid	geographic latitude and longitude
Dashed lines	corrected geomagnetic latitude (epoch 2000.0)
Dotted line	best-fit great circle west coast stations
Blue circles	DMI magnetometer stations
Red circles	MAGIC sites (SPRL, Univ. of Michigan)
Blue triangles	DMI geomagnetic observatories
Full circles	data from preceding day are transmitted to DMI via modem and telephone line (presently every morning around 03 UT)
Open circles	data are stored locally and sent to DMI via snail mail (up to several months delay)
Black Roman	data are transmitted to DMI in near real time (presently every 15 min, in the future possibly more frequently)

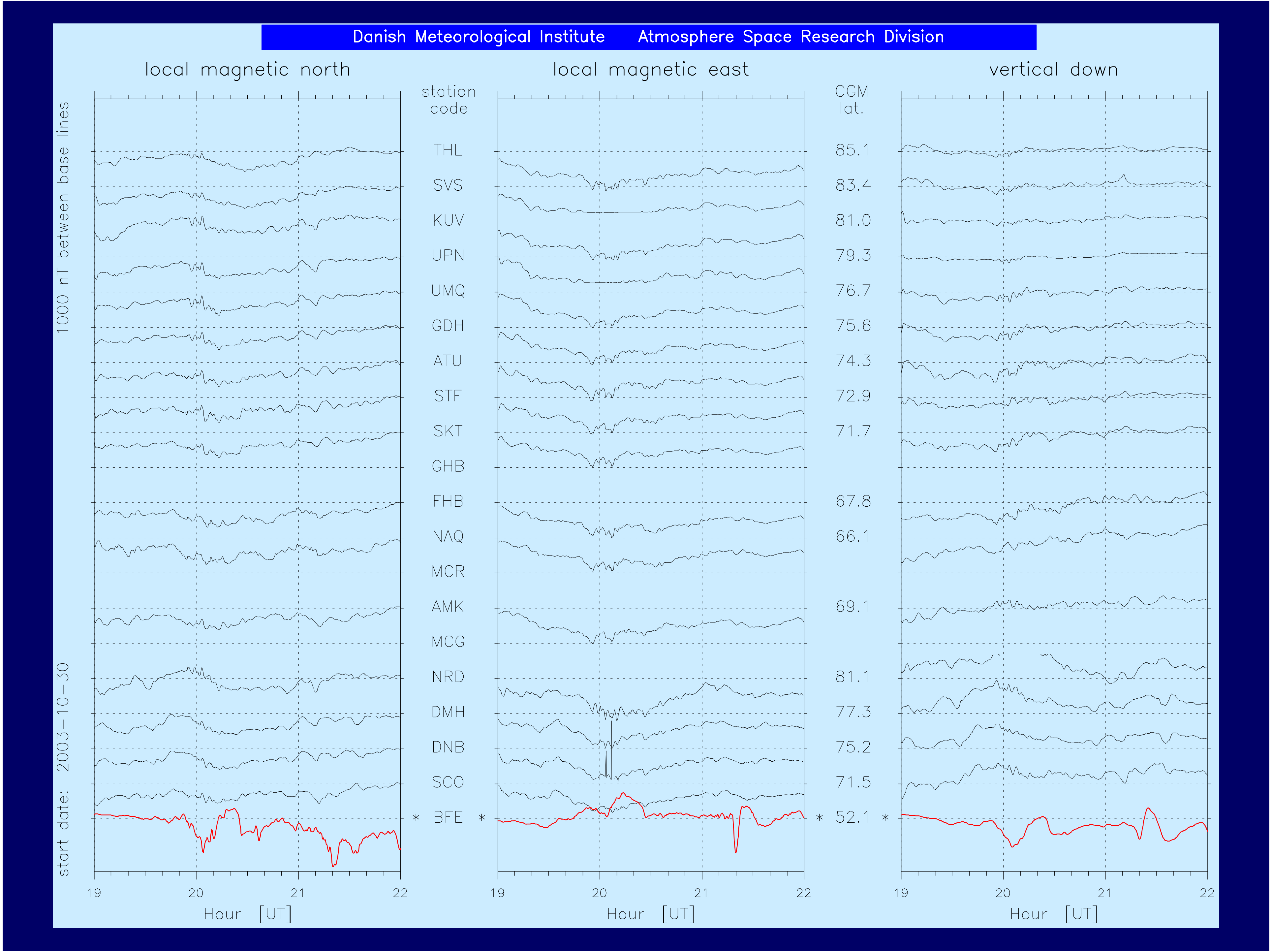

Danish Meteorological Institute Atmosphere Space Research Division
local magnetic north
local magnetic east
vertical down
station code
CGM lat.
1000 nT between base lines
start date: 2003-10-30
THL 85.1
SVS 83.4
KUV 81.0
UPN 79.3
UMQ 76.7
GDH 75.6
ATU 74.3
STF 72.9
SKT 71.7
GHB
FHB 67.8
NAQ 66.1
MCR
AMK 69.1
MCG
NRD 81.1
DMH 77.3
DNB 75.2
SCO 71.5
* BFE * * 52.1 *
19
20
21
22
Hour [UT]

δB/δt (1-s samples) at DMI magnetometer sites

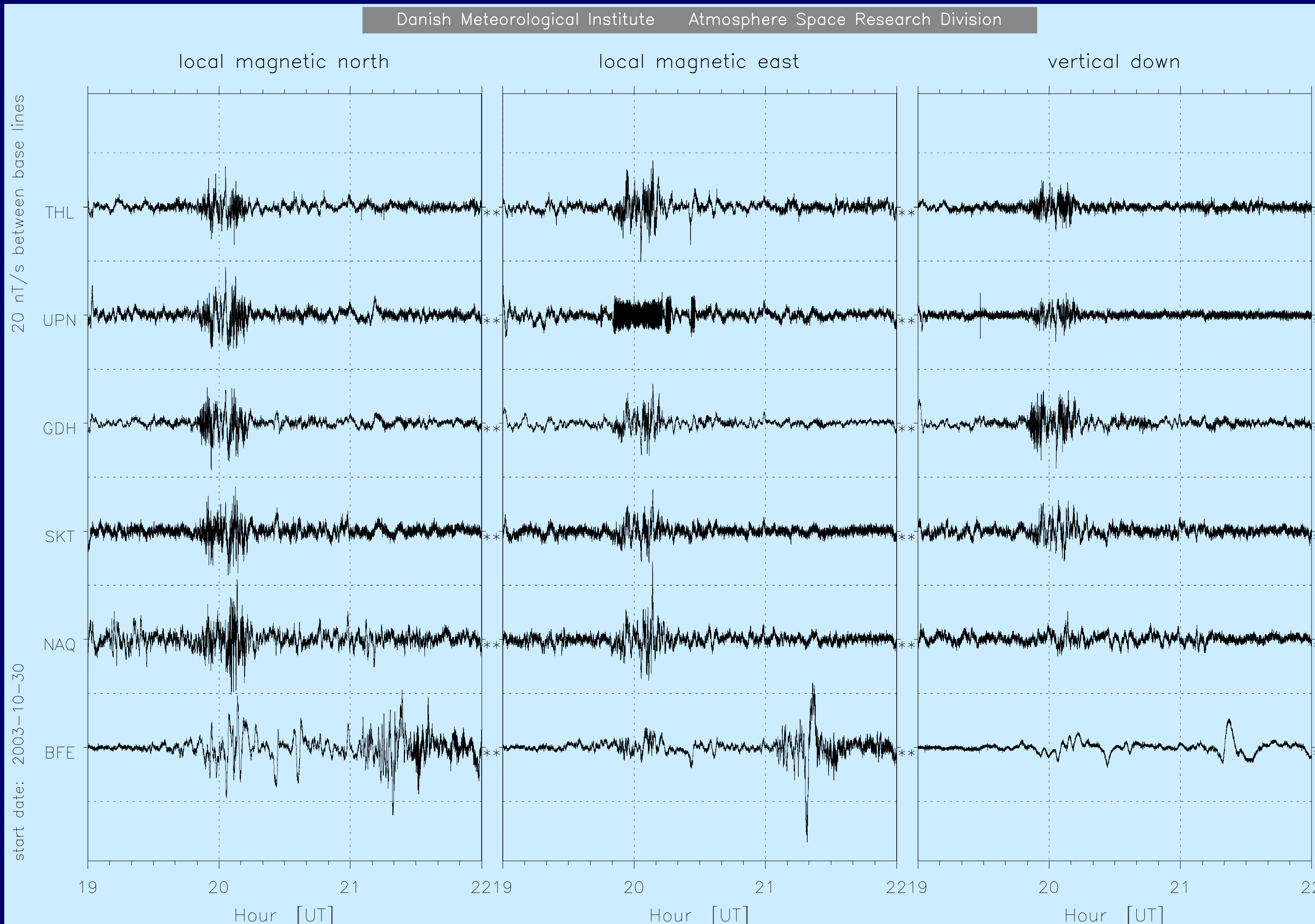

δB/δt [nT/s] – peak values

THL (85.1° cgml)	+8.6 E	-10.1 E	10.3 H	(20:00 – 20:10)
UPN (79.3° cgml)	+8.9 N	-6.5 N	8.9 H	(20:00 – 20:10)
GDH (75.6° cgml)	+7.2 E	-8.8 N	9.9 H	(20:00 – 20:10)
SKT (71.7° cgml)	+8.2 N	-8.1 N	9.0 H	(20:00 – 20:10)
NAQ (66.1° cgml)	+14.4 E	-10.2 N	17.1 H	(20:00 – 20:10)
BFE (52.1° cgml)	+9.6 N	-9.4 N	9.7 H	(20:00 – 20:10)
	+12.0 E	-17.5 E	18.1 H	(≈ 21:20)

Is this latitudinal distribution of amplitude and time derivative typical – or is it exceptional ?

Method

(1) select those days during the the first nine months of 2003 during which DMI's observatories delivered usable 1-s samples virtually over the entire day

(2) remove spikes and jumps and bridge individual invalid data points

(3) apply lowpass filter with 10-s cutoff and subtract daily mean

(4) divide filtered time series into 1-min segments

(5) find in each segment the maximum absolute horizontal deviation from zero level

$$var_k(i) = max \{ \delta H_k^2 (i) + \delta E_k^2 (i) \}^{½}$$

(6) return to the uncorrected and unfiltered time series and compute time derivatives

$$deriv_k (i) = \{ [\delta H_k (i+1) - \delta H_k (i)]^2 + [\delta E_k (i+1) - \delta E_k (i)]^2 \}^{½}$$

(7) bin variances and time derivatives with respect to magnitude (increase bin width with increasing magnitude)

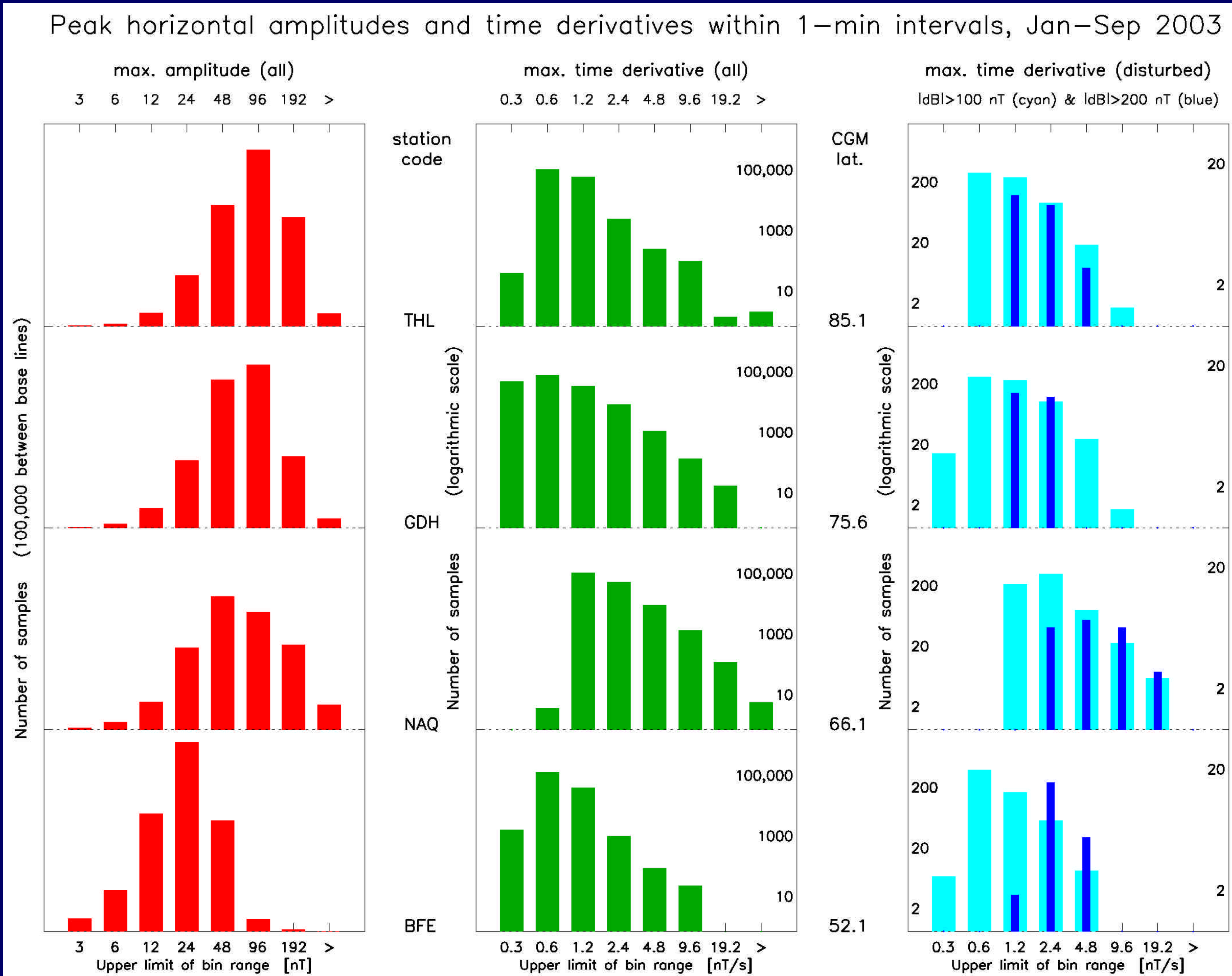
Peak horizontal amplitudes and time derivatives within 1-min intervals, Jan-Sep 2003
max. amplitude (all)
max. time derivative (all)
max. time derivative (disturbed)
|dB|>100 nT (cyan) & |dB|>200 nT (blue)
station code
CGM lat.
THL 85.1
GDH 75.6
NAQ 66.1
BFE 52.1
Number of samples (100,000 between base lines)
Number of samples (logarithmic scale)
100,000
1000
10
200
20
2
3 6 12 24 48 96 192 >
0.3 0.6 1.2 2.4 4.8 9.6 19.2 >
Upper limit of bin range [nT]
Upper limit of bin range [nT/s]

The largest ∂B/∂t values occur during geomagnetic storms

- auroral electrojet expansion and intensification
- ring current intensification
- ssc

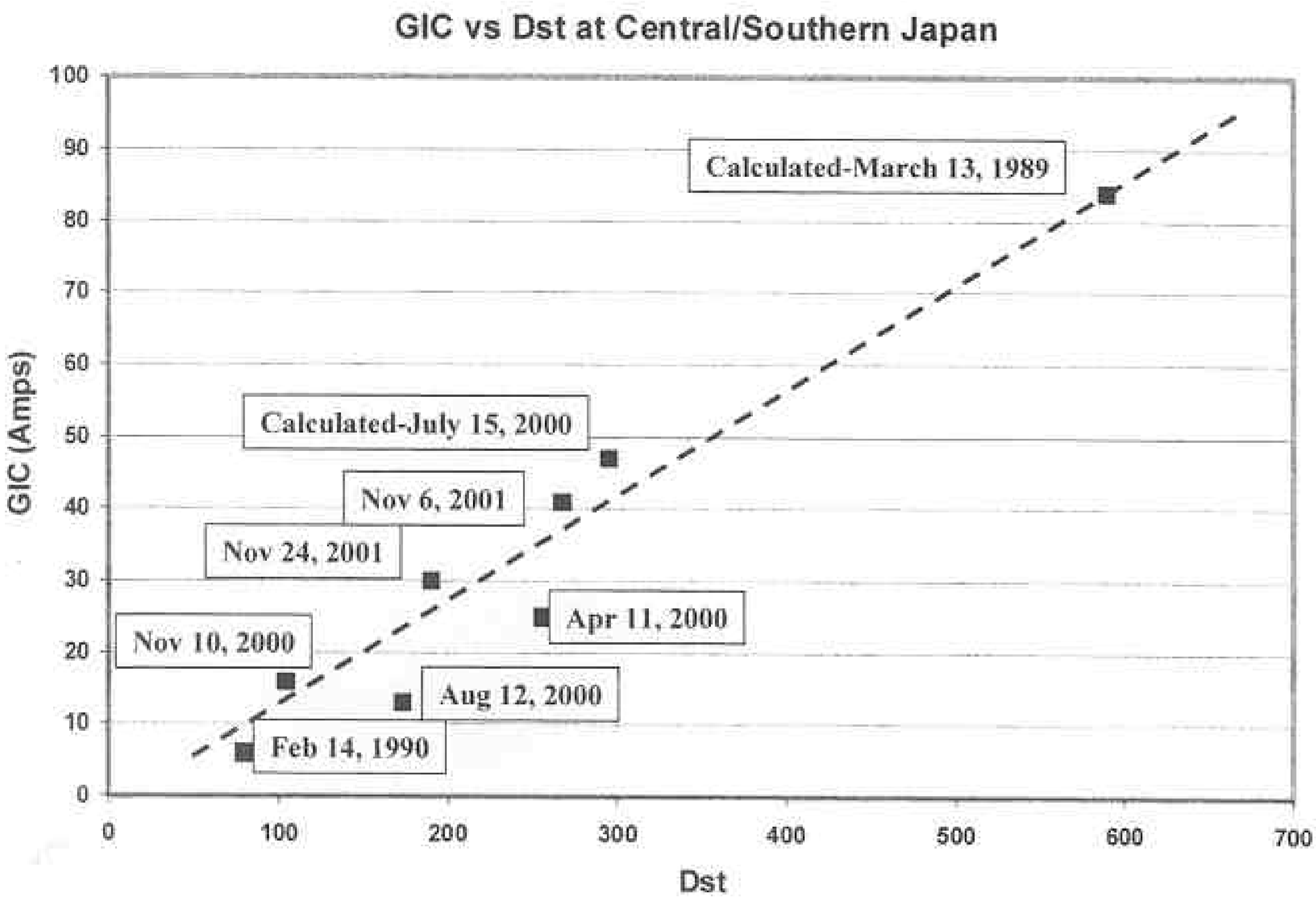

Figure 13. Trend of GIC flows and observed and calculated GIC flows in 500kV transformer in central Japan power grid due to ring current intensification at low latitude locations.

figure from Kappenman, ESPRIT lectures volume, 2004

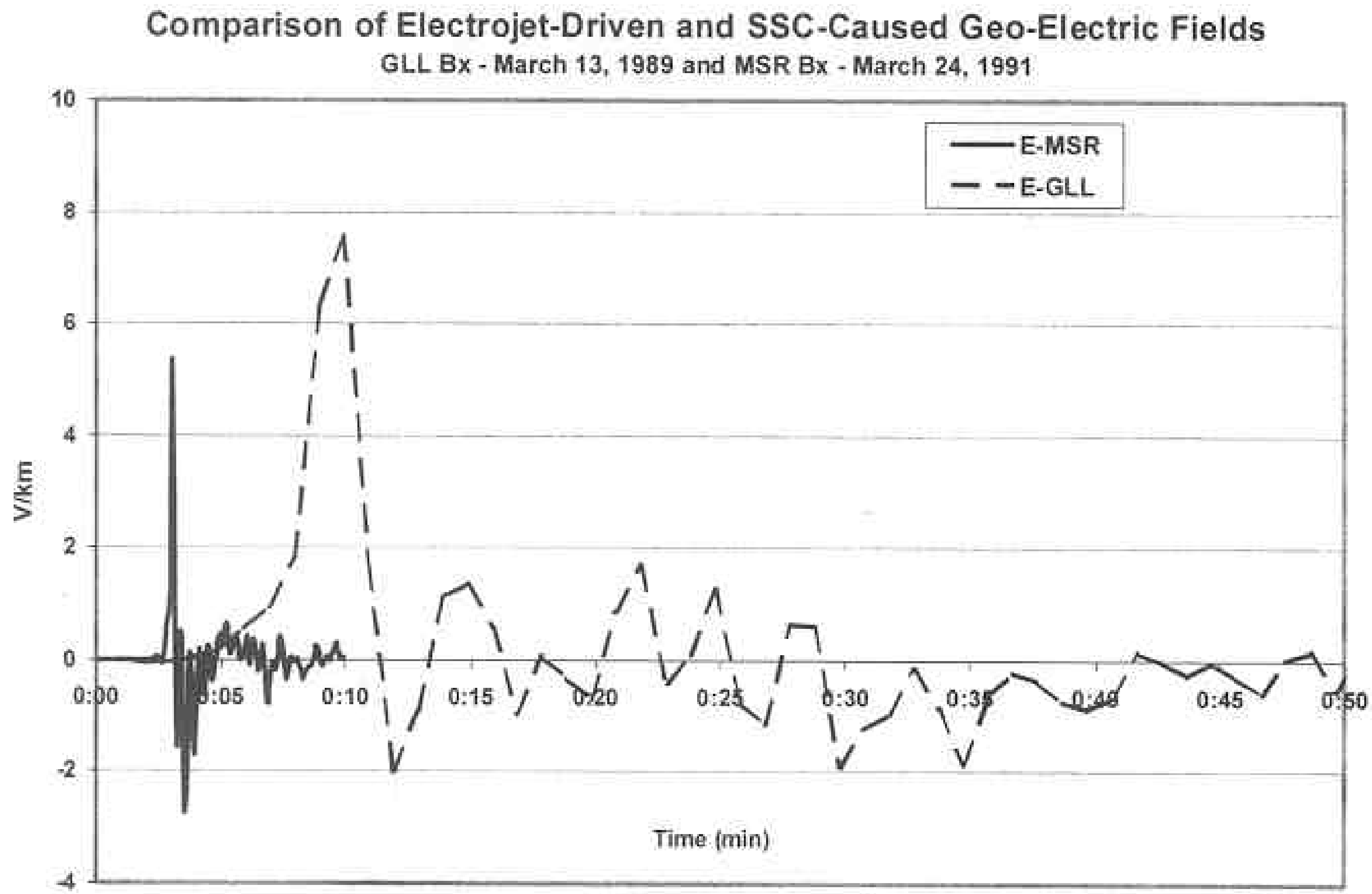

Figure 11. Comparison of estimated geo-electric field from Electrojet-driven disturbance as observed at GLL (March 13, 1989) and from SSC-event as observed at MSR (March 244, 1991).

figure from Kappenman, ESPRIT lectures volume, 2004

Second physics category

equipment sensitive to the amplitude δB

- magnetic anomaly surveys (e.g., aeromagnetic surveys)
- directional well drilling

potential problems caused by geomagnetic variations

(reference field variations)

Magnetic anomaly surveys,
specifically aeromagnetic surveys

operations impeded by

large-amplitude total field variations

Fig. 1. Location of government-financed high-resolution airborne geophysical surveys in the period 1992–1999. Aeromagnetic surveys (Aeromag) are outlined in **red** and combined electromagnetic and magnetic surveys (AEM Greenland) are outlined in **green**. Slightly modified from Rasmussen & Thorning (1999).

figure from Rasmussen and van Gool, GEUS, 2000

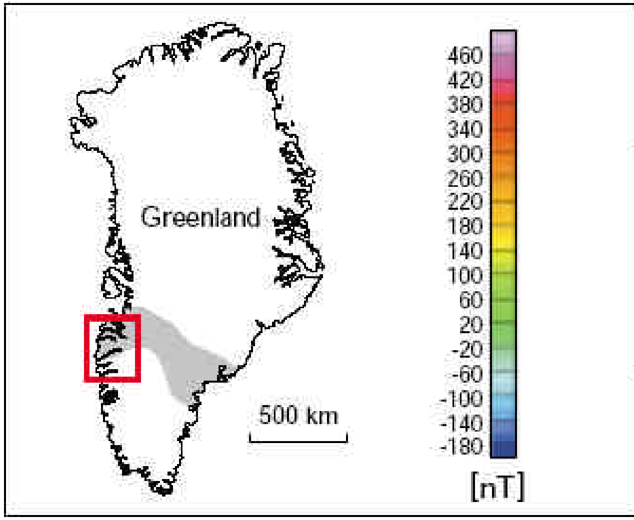

Fig. 2. Magnetic total-field intensity with shaded relief for the region covered by project *Aeromag 1999*. Obtained magnetic anomalies are in the range –1000 nT to 2000 nT. **Dotted lines**: boundaries of the segments and belts of the Nagssugtoqidian orogen as discussed in the text, **closely spaced dots** indicate boundaries mapped in the field, **wider-spaced dots** indicate extrapolations based on the aeromagnetic data. For explanation of **NNO**, **CNO** and **SNO** see Fig. 3. **SC**: Sarfartoq carbonatite; **K**: Kangerlussuaq airport. **Shading** on the inset map shows the regional extent of the Nagssugtoqidian orogen.

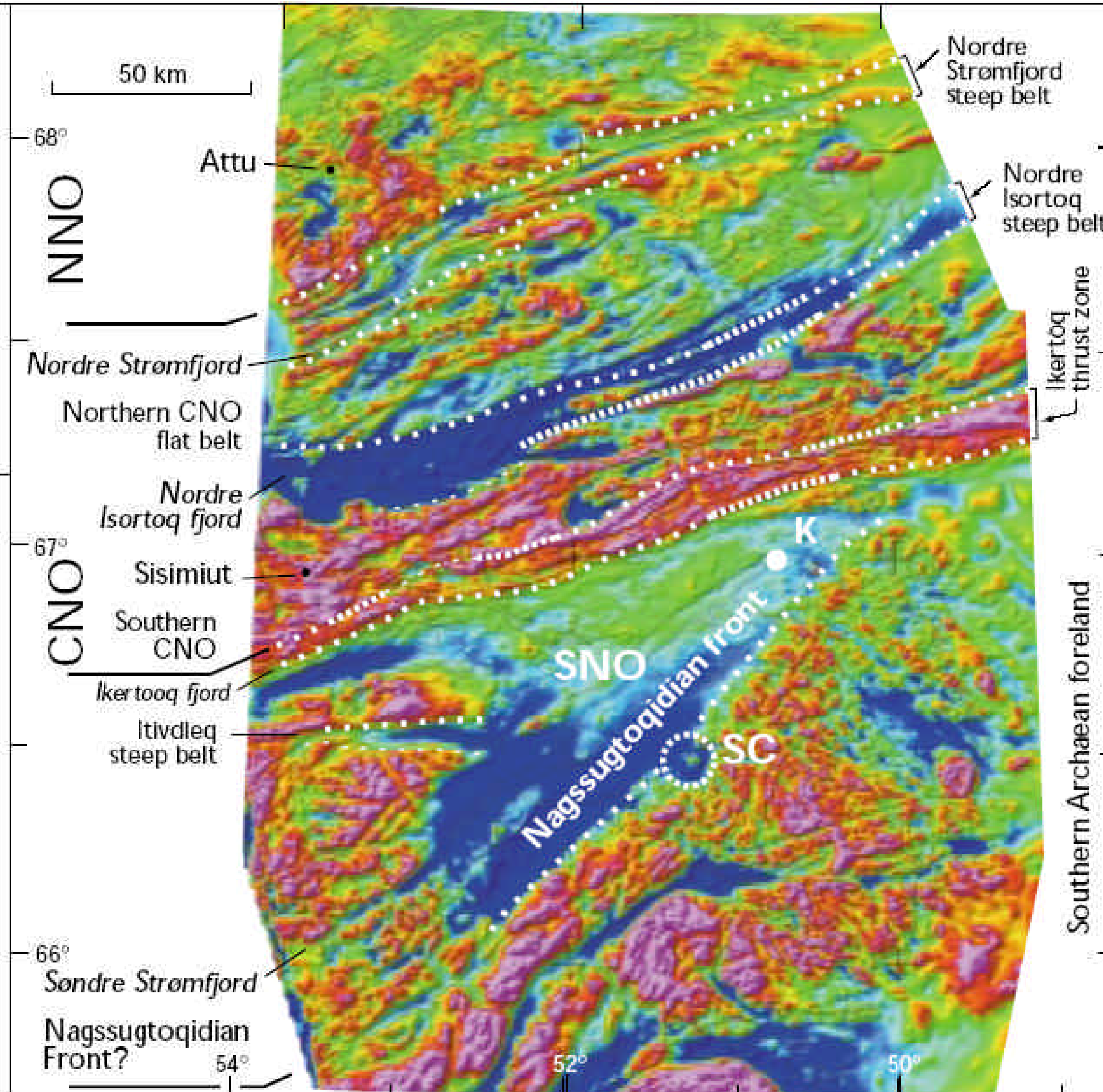

figure from Rasmussen and van Gool, GEUS, 2000

How does the magnitude of magnetostatic anomalies compare to the amplitude of geomagnetic variations ?

Method

(1) select those days during the the first nine months of 2003 during which DMI's observatories delivered usable 1-s samples virtually over the entire day

(2) remove spikes and jumps and bridge individual invalid data points

(3) apply lowpass filter with 10-s cutoff and subtract daily mean

(4) divide filtered time series into 1-min segments

(5) find in each segment the maximum absolute total field deviation from zero level

$$var_k(i) = max\ \{ \delta H_k^2\,(i) \cdot cos^2(I_k) + \delta Z_k^2\,(i) \cdot sin^2(I_k) \}^{1/2}$$

(6) find the number of 1-min intervals where at least one data point exceeds 100 nT and 200 nT, respectively

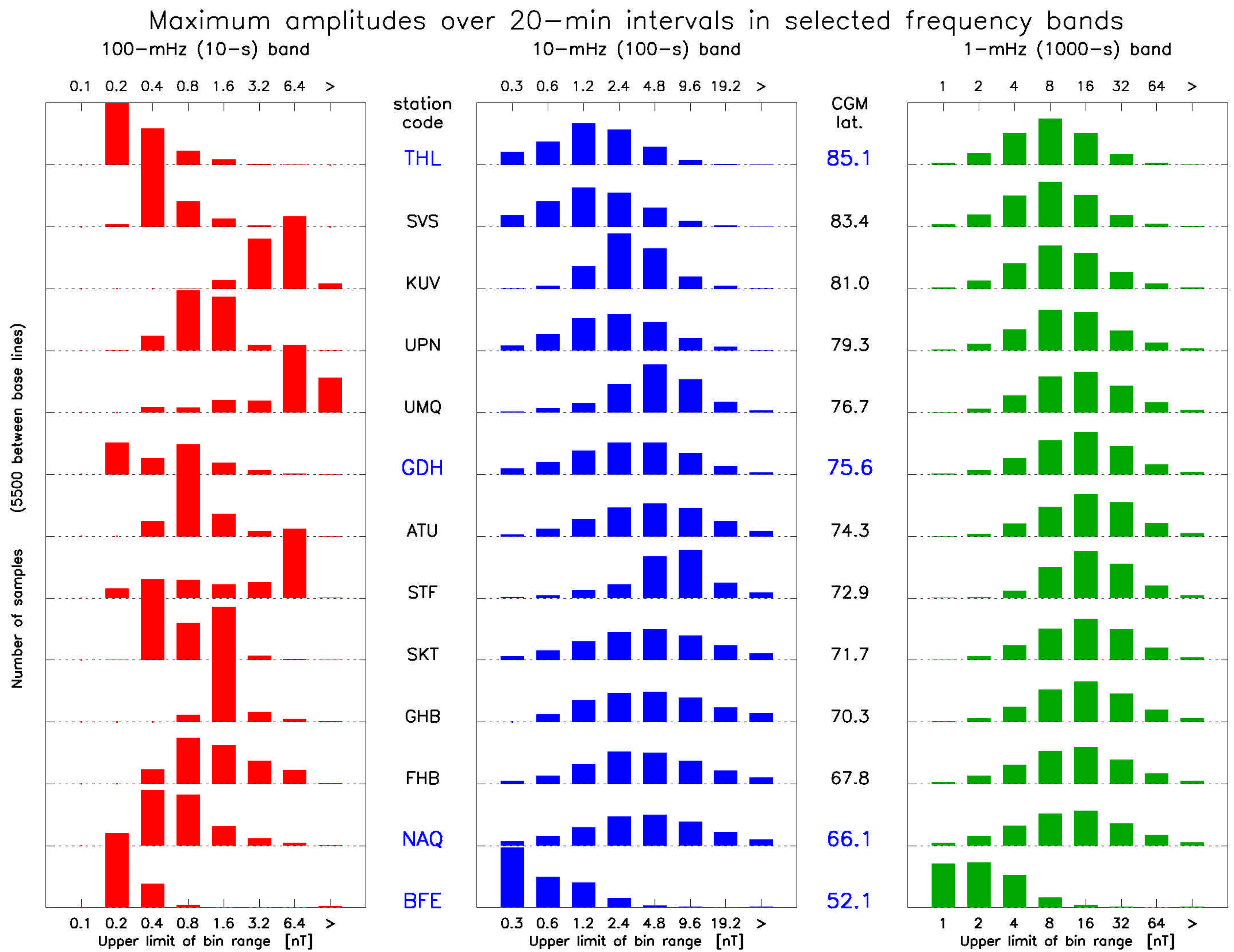
Maximum amplitudes over 20–min intervals in selected frequency bands
100–mHz (10–s) band
10–mHz (100–s) band
1–mHz (1000–s) band
0.1 0.2 0.4 0.8 1.6 3.2 6.4 >
0.3 0.6 1.2 2.4 4.8 9.6 19.2 >
1 2 4 8 16 32 64 >
station code
CGM lat.
THL 85.1
SVS 83.4
KUV 81.0
UPN 79.3
UMQ 76.7
GDH 75.6
ATU 74.3
STF 72.9
SKT 71.7
GHB 70.3
FHB 67.8
NAQ 66.1
BFE 52.1
Number of samples (5500 between base lines)
Upper limit of bin range [nT]

Sample case: West Greenland

magnetostatic total field anomaly range: –200 to +500 nT

relative number of 1-min intervals in which the total field deviation exceeds ±100 nT and ±200 nT, respectively

		±100 nT	±200 nT
THL	(85.1° cgml)	3.6%	0.3 %
GDH	(75.6° cgml)	20.0%	2.6 %
NAQ	(66.1° cgml)	8.6%	1.2 %
BFE	(52.1° cgml)	0.1%	.03 %

Directional well drilling

controlled by borehead magnetometers

operations impeded by

long-lasting large-amplitude total field variations

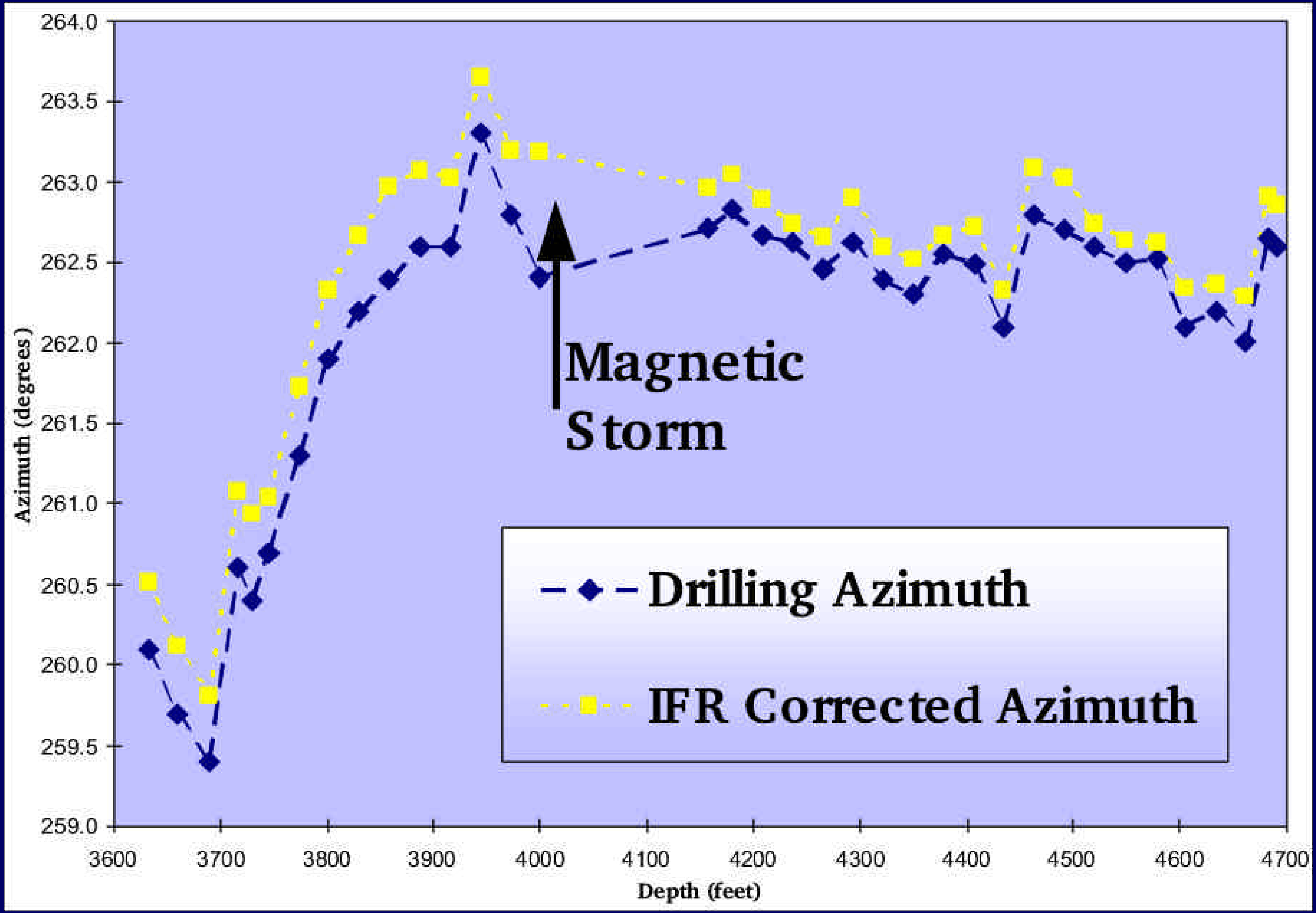

figure from Clark and Clarke, SWW ESTEC, 2001

Diurnal distribution of the largest 0.2% of ~20 years of geomagnetic field variations

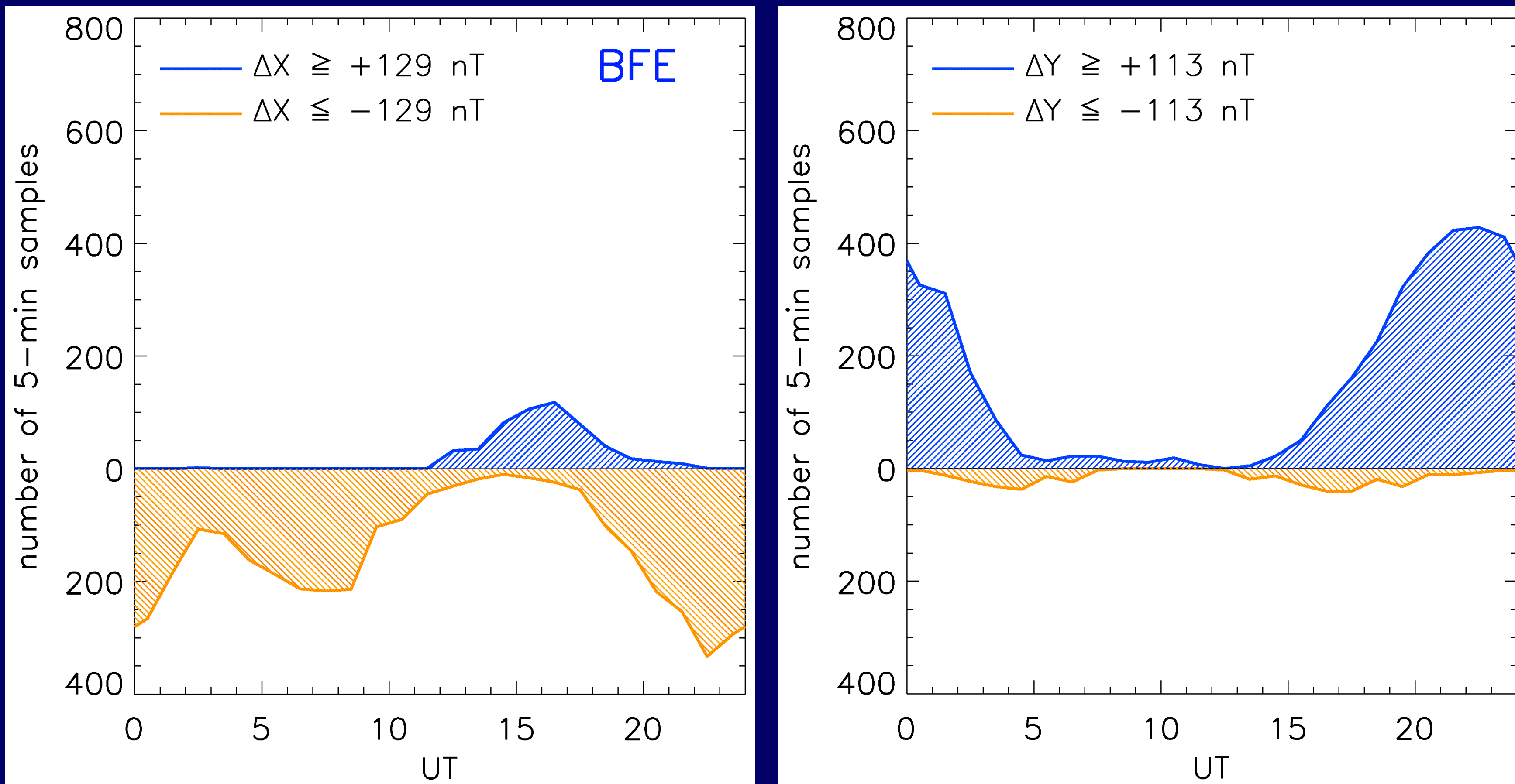

figures provided by H. Gleisner, 2004

Qualitative risk assessment

- Statistically, the polar cap (>73°) is subject to the largest δB.
- Statistically, the nominal auroral zone (~66° cgml) is subject to the largest $\partial B/\partial t$, even under severe storm conditions when the largest δB may occur at subauroral latitudes.
- Magnetic anomaly surveys and directional well-drilling activities are affected by large δB.
- Electric power networks, pipelines and telecommunication cables are sensitive to $\partial B/\partial t$.
- The most damaging GIC effects occur in large electric power grids. Pipelines and transoceanic cables are of lesser concern.
- Large magnetic field variations are annoying for drilling and surveying but not directly damaging